Rapid Kinetics of α_2-Adrenergic Inhibition of Adenylate Cyclase. Evidence for a Distal Rate-Limiting Step†

William J. Thomsen‡ and Richard R. Neubig*,‡,§

Departments of Pharmacology and Internal Medicine (Hypertension Division), University of Michigan, Ann Arbor, Michigan 48109-0626

Received March 27, 1989; Revised Manuscript Received June 13, 1989

ABSTRACT: Activation and inhibition of adenylate cyclase in the presence of GTP, the natural guanine nucleotide regulator, are too fast to study by standard biochemical methods. In order to identify the rate-limiting steps in adenylate cyclase regulation, we measured the kinetics of stimulation and inhibition of the enzyme on a subsecond to second time scale using a novel rapid-mix quench technique. Even using our rapid-mix quench method, activation by PGE_1 and forskolin was instantaneous (cAMP accumulation was linear between 0.5 and 30 s). In contrast, we found a lag period of 1.2–10 s for epinephrine-mediated inhibition. The length of the lag depended on the concentration of GTP and monovalent cations present. In the absence of NaCl, the rate constant for the onset of inhibition (k_{inh}) increased only slightly with GTP concentration saturating at a value of 0.16 s^{-1} ($t_{1/2}$ 4.3 s) at 1 μM GTP. In the presence of 100 mM NaCl, k_{inh} was strongly dependent on GTP concentration, reaching a maximum value of 0.57 s^{-1} ($t_{1/2}$ 1.2 s) at 100 μM GTP. Thus, activation of both G_i and G_s in intact platelet membranes is much faster ($t_{1/2} < 5$ s) than previously reported for reconstituted systems. Also, the strong dependence of the rate of adenylate cyclase inhibition on GTP concentration implies that the rate-limiting step in inhibition is distal to GTP binding. The effect of NaCl to increase the maximal rate of inhibition is specific for sodium since KCl has no effect on k_{inh}. In contrast, both sodium and potassium chloride increased the steady-state EC_{50} for epinephrine and GTP while neither affected the maximum percentage inhibition. We used these kinetic and steady-state data to test several models of α_2-receptor and G_i-mediated adenylate cyclase inhibition in a quantitative manner. Two distinct models gave similar fits of experimental data in the absence of NaCl. In one, the rate-limiting step is GDP release while in the other, activation of the GTP-liganded G protein is limiting. Only the latter model also explains our prior observation that preincubation of platelet membranes with α_2 agonist in the absence of GTP increases the potency for inhibition [Thomsen et al. (1988) *Mol. Pharmacol. 34*, 814–822]. Thus, both in the presence and in the absence of sodium chloride, the conformational change of GTP-liganded G_i rather than GDP release is rate limiting. According to this model, sodium chloride increases the rate of three reaction steps: (1) agonist dissociation from receptor; (2) GTP dissociation from G_i; and (3) the rate-limiting conformational change of GTP-liganded G protein. The rapid kinetic studies reported here provide new information regarding regulation of adenylate cyclase by sodium chloride and the natural nucleotide regulator, GTP.

Agonist binding to α_2-adrenergic receptors results in inhibition of adenylate cyclase (Limbird, 1981) and activation of other cellular responses such as phospholipases and ion channels (Limbird, 1988). These responses involve at least three distinct proteins: the α_2-receptor itself, an inhibitory guanine nucleotide binding protein termed G_i[1] and the catalytic subunit of adenylate cyclase or other effector enzyme (Gilman, 1987). Because of the number of components and the complex nature of their interactions, the exact molecular mechanism of agonist-mediated G protein activation remains unclear.

Studies of the *transient* kinetics of hormone and guanine nucleotide mediated stimulation and inhibition of adenylate cyclase using plasma membrane preparations have contributed to our understanding of the mechanism of these processes. Both stimulation and inhibition of adenylate cyclase by non-hydrolyzable guanine nucleotide analogues occur after a lag period on the order of minutes (Tolkovsky & Levitzki, 1978; Steer & Wood, 1979; Tolkovsky et al., 1982; Jakobs & Aktories, 1983). In contrast, when GTP, the natural nucleotide regulator, is used, the kinetics of agonist-mediated stimulation (Birnbaumer & Pohl, 1973; Sonne et al., 1978) and inhibition (Jakobs, 1979; Jakobs et al., 1984a,b) of adenylate cyclase are too fast to quantitate by manual methods [see, however, Rodbell et al. (1974)].

A major advance in the study of these receptor G protein systems has been the reconstitution of purified receptors with G_s and G_i (Brandt & Ross, 1985; Tota et al., 1987). Kinetic studies in these reconstituted systems (Brandt & Ross, 1985, 1986; May & Ross, 1988; Tota et al., 1987) found rates of GDP release and GTP binding of $\approx$1 min^{-1} and a rate of GTP hydrolysis of 2–4 min^{-1}. These investigators proposed that the hormone–receptor complex induces an open state of the G protein, which allows nucleotide exchange to occur.

† This work was supported by NSF Grant DCB-8409333 and NIH Grants HL 37551 and GM 39561. W.J.T. is a Horace H. Rackham predoctoral fellow. R.R.N. is an AHA/Genentech Inc. Established Investigator.

* Address correspondence to this author at the Department of Pharmacology, M6322 Medical Science Building I, Ann Arbor, MI 48109-0626.

‡ Department of Pharmacology.

§ Department of Internal Medicine.

[1] Abbreviations: G_i, the inhibitory guanine nucleotide binding protein; G_s, the stimulatory guanine nucleotide binding protein; G_o the "other" guanine nucleotide binding protein isolated from brain; UK 14 304, 5-bromo-*N*-(4,5-dihydro-1*H*-imidazol-2-yl)-6-quinoxalinamine; DTT, dithiothreitol.

0006-2960/89/0428-8778$01.50/0

The surprisingly slow rates of these processes in reconstituted systems are hard to reconcile with the rapid activation of adenylate cyclase in membranes [see Casey and Gilman (1988)]. The activation and deactivation of other G proteins such as transducin (Wagner et al., 1988; Sitaramayya et al., 1988) and the G_i-like protein coupled to cardiac K^+ channels (Breitwieser & Szabo, 1988; Okabe et al., 1989) also occur on the second rather than the minute time scale. These discrepancies prompted us to examine the kinetics of adenylate cyclase stimulation and inhibition in native platelet membranes.

To study the rates of α_2-agonist-mediated inhibition of platelet membrane adenylate cyclase in the presence of GTP, we have used rapid-mix quench methods (Chance, 1974; Fersht & Jakes, 1975; Neubig et al., 1982). Using this method, we were able to quantitate stimulation and inhibition of platelet membrane adenylate cyclase on a subsecond to second time scale.

Materials and Methods

Materials. [α-^{32}P]ATP and [^{3}H]cAMP were purchased from Amersham Corp. Forskolin was obtained from Calbiochem-Behring. All other chemicals were reagent grade or better from standard suppliers. Purified human platelet plasma membranes were prepared as described by Neubig and Szamraj (1986) with modifications (Neubig et al., 1988).

Manual Measurement of Adenylate Cyclase Activity. Assays were performed as previously described (Thomsen et al., 1988). To exclude Na^+ from the assay, Tris salts of ATP, GTP, EGTA, and creatine phosphate and free ascorbic acid were used. All incubations contained 10 μM forskolin and 0.05–0.15 mg of membrane protein per 100 μL. The tubes were incubated for 15 min at 30 °C, and then [^{32}P]cAMP was measured by the method of Salomon et al. (1974). Blanks were determined by mixing membranes with stop solution before adding [α-^{32}P]ATP and other reagents. Blank values ranged from 60 to 90 cpm.

Rapid-Mix Quench Measurement of Adenylate Cyclase Stimulation and Inhibition. The time course of PGE_1- and forskolin-mediated stimulation and epinephrine-mediated inhibition of adenylate cyclase activity was measured between 0.5 and 60 s using a rapid-mix quench apparatus recently described for measurement of α_2-agonist binding (Neubig & Thomsen, 1987). The design of this instrument was similar to a pulsed-quench apparatus previously described (Neubig et al., 1982; Neubig, 1980), except that stainless-steel fittings, valves, and tubing are used. Hamilton syringes (0.5 mL) and tubing are in a water bath controlled at 30 °C by a Haake circulating pump. An IBM-PC computer with a Tecmar Labmaster board controls a 12V Autochrom selenoid controller, regulating air pressure to Bimba air-driven rams and a Valco 10 port HPLC valve. An analog-to-digital converter measures the output of linear potentiometers attached to the two rams to monitor the syringe drivers. To initiate the adenylate cyclase assay, compressed air forces the first ram down on two syringes, forcing 100 μL of platelet membranes and 100 μL of reaction cocktail into an aging tube. The final concentrations in the reaction mixture are as follows: Tris-HCl, 25 mM; $MgCl_2$, 2.5 mM; EGTA, 1.5 mM; DTT, 0.5 mM; cAMP, 1 mM; isobutylmethylxanthine, 0.01 mM; GTP, 10 μM (unless stated); phosphocreatine, 5 mM; creatine phosphokinase, 50 units/mL; propranolol, 10 μM; ATP, 0.2 mM (0.5–1 μCi of [α-^{32}P]ATP/tube), plus the indicated concentrations of drugs and monovalent ions. Incubations including epinephrine and the paired controls also contained 0.01% ascorbic acid. At the indicated times, the second ram forces the incubation mixture out of the aging tube, mixing

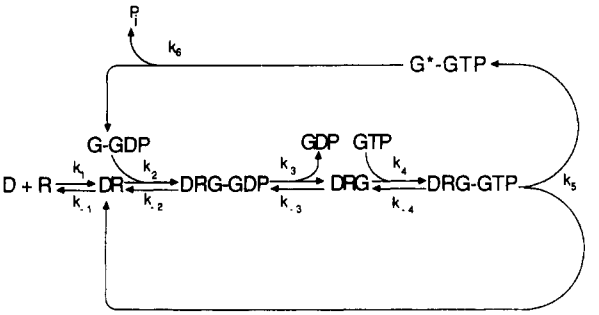

FIGURE 1: Kinetic model of α_2-agonist-mediated inhibition of platelet membrane adenylate cyclase. D and R represent free agonist and α_2-receptor which combine to form the complex DR. interaction of agonist and receptor facilitates the formation of a ternary complex between agonist, receptor, and GDP-liganded G protein designated as DRG–GDP. This results in the release of GDP to form the high-affinity ternary complex (DRG) which then binds GTP to form DRG–GTP. GTP binding promotes dissociation of this complex to form activated G protein, G*–GTP, and the low-affinity complex, DR. The inhibition of adenylate cyclase is assumed to be proportional to the concentration of G*–GTP formed (see Discussion). The inhibitory cycle is terminated by the hydrolysis of GTP to GDP, restoring G_i to an inactive GDP-liganded form. The inhibitory cycle continues in the sustained presence of agonist and GTP. The values for the rate constants for each step in the model are listed in Table II.

it with quench solution (final concentrations: 1% SDS, 5 mM ATP, and 0.5 mM cAMP). The quenched reaction mixture is collected in tubes containing 20000–60000 cpm [^{3}H]cAMP as a recovery standard. All incubations contained 10 μM forskolin (except basal and PGE_1 time course studies) and 0.05–0.10 mg of membrane protein per tube, as determined by the method of Lowry et al. (1951). [^{32}P]cAMP formed was measured as described above. Radioactivity was determined by scintillation counting for 20 min to reduce the contribution of counting error. Blanks determined by mixing 100 μL of membrane with 200 μL of stop solution before adding [α-^{32}P]ATP and other reaction ingredients gave values between 60 and 90 cpm.

Data Analysis. For analysis of the kinetics of epinephrine-mediated inhibition of adenylate cyclase, the percentage reduction in cAMP produced was calculated from the samples without and with epinephrine at each time point and plotted vs time. The values were fitted to a single-exponential function by a nonlinear least-squares curve-fitting program (GraphPAD, ISI) which provided estimates of the rate constants of inhibition (k_{inh}) and maximal levels of epinephrine-mediated inhibition of adenylate cyclase. EC_{50} values from epinephrine and GTP dose–response data were determined by fitting data to a log dose–response function using the same nonlinear least-squares fitting program.

Simulations of the Kinetic Model of G Protein Activation. The theoretical time course of α_2-receptor-mediated G protein activation was simulated on an ATT Unix or a Micro VAX using the SAAM 29 kinetic modeling program (Foster & Boston, 1979) as described previously (Thomsen et al., 1988). The concentration of active G protein (G*–GTP) was simulated for times between 0.5 s and 15 min according to the kinetic model indicated in Figure 1. Initial simulations utilized the same kinetic parameters as in our earlier report (Thomsen et al., 1988; and see parameter set A, Table II). The parameters were varied with the SAAM 29 kinetic modeling program to obtain a minimum sum of the squared residuals (SSR) between theory and experimental data. Both kinetic and steady-state data were analyzed simultaneously in determining the optimal kinetic parameters. The complete data set included time course data at six different GTP concentrations (mini-

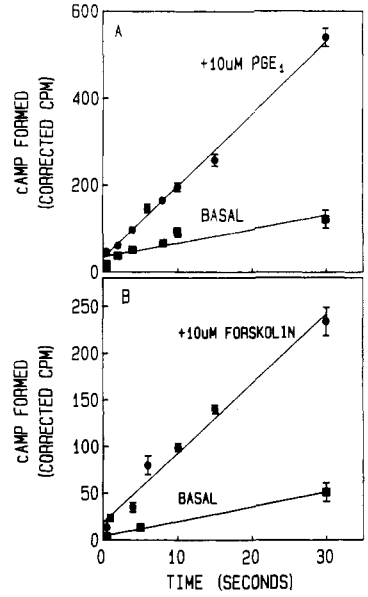

FIGURE 2: Rapid time course of PGE_1- and forskolin-mediated stimulation of platelet membrane adenylate cyclase. The time course of [^{32}P]cAMP production at 30 °C was measured by using the rapid-mix quench method described under Materials and Methods. Membranes were prewarmed for 3–5 min in buffer containing 50 mM Tris-HCl, 5 mM $MgCl_2$, 3 mM EGTA, and 1 mM DTT, pH 7.6. All reactions were in 200 μL and contained 0.05–0.15 mg of platelet membrane protein per tube, 1 μM GTP, 100 mM NaCl, and additional reagents as described under Materials and Methods. (A) The time course of accumulation of [^{32}P]cAMP in the presence (●) and absence (■) of 10 μM PGE_1 is shown. (B) The time course of accumulation of cAMP in the presence (●) and absence (■) of 10 μM forskolin is shown. To improve scintillation counting statistics for samples with low levels of [^{32}P]cAMP, 20-min counts were done. All data are expressed as counts of [^{32}P]cAMP formed, corrected for recovery (50–80%) after subtracting blank counts (70 ± 20 cpm). Data points represent the mean ± SEM for quadruplicate (A) and mean ± range of duplicate (B) determinations. Lines through data are linear regressions.

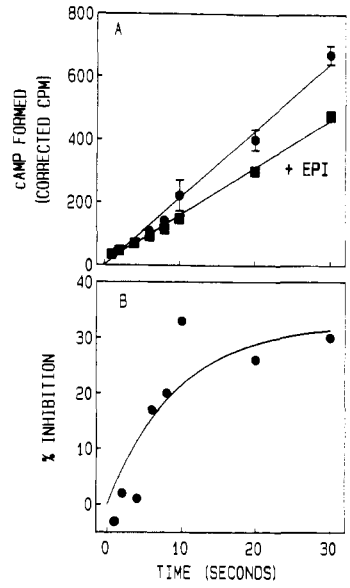

FIGURE 3: Rapid time course of inhibition of forskolin-activated adenylate cyclase by epinephrine. (A) The accumulation of [^{32}P]-cAMP at times of 1–60 s was measured in the presence (■) and absence (●) of 100 μM epinephrine. Assays contained 10 μM GTP and 100 mM NaCl and other reagents described under Materials and Methods. Each data point represents the mean ± SEM of quadruplicate determinations for a single experiment. Lines through data are linear regressions of the data. (B) The percent inhibition at each time point was determined from data in (A) and plotted versus time. Data were fit to a monoexponential function by the nonlinear least-squares curve-fitting program described under Materials and Methods.

mum of eight time points per concentration) and steady-state agonist and GTP dose–response data (eight concentrations each). Because the maximal adenylate cyclase inhibition was variable in the rapid kinetic experiments, the amplitude of inhibition in the kinetic simulations was fit separately for each experiment rather than being constrained by the model. Therefore, the kinetic data were fit on the basis of the time course and not the maximal percentage inhibition. Amplitude information in the fits was provided by the steady-state dose–response experiments. Optimization of the kinetic parameters was done by manually varying parameters to obtain a minimum SSR since automated fitting did not reliably find global minima. Because of the long time required for each simulation (approximately 25 min), we were not able to determine the parameters to an accuracy of better than a factor of 2.

RESULTS

Rapid Kinetics of PGE_1- and Forskolin-Mediated Stimulation of Platelet Membrane Adenylate Cyclase. The rapid-mix quench apparatus was used to measure [^{32}P]cAMP accumulation with and without 10 μM PGE_1 on a 0.5–30 s time scale (Figure 2A). Basal activity over this period is significant at the earliest time point (10–20 cpm over blanks) and remains linear over this period. Stimulation of adenylate cyclase mediated by 10 μM PGE_1 in the presence of 1 μM GTP and 100 mM NaCl is immediate in onset, and [^{32}P]cAMP accumulation is linear during this period. By manual methods, PGE_1-stimulated activity is also linear between 0.5 and 15 min (data not shown). [^{32}P]cAMP counts resulting from incubations with PGE_1 are 20–40 counts over basal counts after a 0.5-s incubation, indicating that measurable stimulation occurs at this early time.

Adenylate cyclase stimulation by 10 μM forskolin in the presence of 1 μM GTP and 100 mM NaCl has also occurred by 0.5 s, and cAMP accumulation is linear up to 30 s of incubation (Figure 2B). However, at later time points, forskolin-mediated stimulation of adenylate cyclase is biphasic with steady state achieved by 1–2 min of incubation (Green & and Clark, 1982; Thomsen, 1989). Consistent with this slow phase of forskolin activation, the initial rate obtained from data at 0.5–30 s is typically 70–80% of the steady-state activity from 2–15 min. The minute time scale lag in forskolin-mediated stimulation of adenylate cyclase is not influenced by inclusion of NaCl or by variations of GTP concentration between 0.1 and 100 μM (data not shown).

Rapid Kinetics of Epinephrine-Mediated Inhibition of Forskolin-Stimulated Adenylate Cyclase. The rapid-mix quench method was also used to characterize the kinetics of epinephrine-mediated inhibition of forskolin-activated adenylate cyclase. Even under optimal conditions (100 μM epinephrine and 10 μM GTP), inhibition is not instantaneous (Figure 3A). To obtain an estimate of the rate constant for inhibition (k_{inh}), the percent inhibition at each time was calculated and plotted against time. Such data were fit to a monoexponential function by using a nonlinear least-squares curve-fitting program described under Materials and Methods and are shown in Figure 3B. The rate constant for the onset of inhibition, k_{inh}, was 0.12 s^{-1}, which corresponds to a $t_{1/2}$ of 6 s. Because of the scatter in the time course data and the relatively low levels of [^{32}P]cAMP formed at early times, multiple experiments each with quadruplicate determinations were pooled in the subsequent analysis.

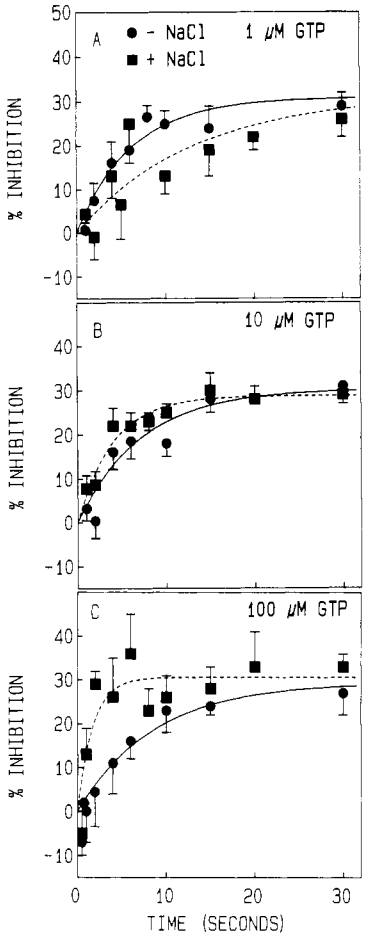

FIGURE 4: Effect of NaCl on the rapid time course of adenylate cyclase inhibition by epinephrine. Pooled data for the time course of epinephrine-mediated inhibition of forskolin-stimulated adenylate cyclase are shown in the presence (■) and absence (●) of 100 mM NaCl for (A) 1 μM, (B) 10 μM, and (C) 100 μM GTP. All data were obtained by using the rapid-mix apparatus described under Materials and Methods. At each time for each experiment, the percentage inhibition was calculated, and the results for three to nine experiments each done in quadruplicate were averaged and plotted. Data are mean ± SEM. Results for 10 and 100 μM epinephrine were pooled because the kinetics of inhibition were identical. Lines represent nonlinear least-squares fits of data to a monoexponential function using a curve-fitting program described under Materials and Methods.

To test the role of GDP release vs. GTP binding or distal steps in the rate-limiting step in the α_2 response, the time course of inhibition was evaluated in the presece of different GTP concentrations with and without 100 mM NaCl (Figure 4). In the absence of NaCl, the onset of inhibition was not different for GTP concentrations between 1 and 100 μM. In contrast, the rate of inhibition in the presence of 100 mM NaCl increased strongly with GTP concentration. Rate constants for inhibition of forskolin-stimulated adenylate cyclase (k_{inh}) were determined from the data shown in Figure 4 and similar experiments. The relation of k_{inh} to GTP concentration in the absence and presence of NaCl is more clearly shown in Figure 5. These results indicate that NaCl has two effects on the kinetics of inhibition of adenylate cyclase mediated by saturating concentrations of epinephrine. First, k_{inh} becomes dependent on the concentration of GTP present. Second, the rate of inhibition is significantly increased in the presence of higher GTP concentrations.

The effects of NaCl on the kinetics of α_2-agonist-mediated inhibition appear to be specific for the presence of Na^+ ion. Addition of 100 mM KCl instead of NaCl gave a k_{inh} value of 0.12 ± 0.04 s^{-1} in the presence of 30 μM GTP (data not shown). This value is much closer to the value of 0.10 ± 0.05 s^{-1} in the absence of NaCl than that of 0.40 ± 0.15 s^{-1} seen with 100 mM NaCl. Thus, the influence of NaCl on the *kinetics* of α_2-agonist-mediated inhibition is not due to an alteration of ionic strength or due to Cl^- ion but is specific for the sodium ion.

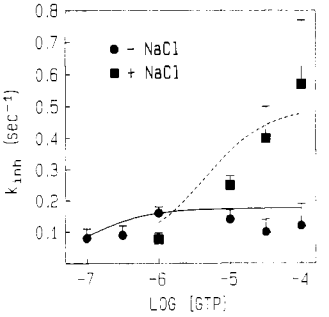

FIGURE 5: Comparison of experimental and theoretical values for k_{inh} in the absence and presence of NaCl. Experimental rate constants for the onset of inhibition (k_{inh}) were determined for each individual experiment represented in Figure 4 and similar experiments. Measurements were from 0.5 to 60 s, and each value of k_{inh} represents the mean ± SEM of values obtained from three to nine separate experiments in which quadruplicate determinations were made at each time point. Results are shown for data without (●) and with (■) 100 mM NaCl. Curves represent theoretical rate constants obtained from simulations of our model using parameter set C (solid line) and set D (dashed line). See Table II for parameter values.

Table I: Comparison of Experimental and Theoretical EC_{50}'s[a]

	experimental EC_{50} (nM)	theoretical EC_{50} (nM)		
		set B	set C	set D
epinephrine - NaCl	55 ± 2	66	55	
epinephrine + 100 mM NaCl	1600 ± 24			1500
epinephrine + 100 mM KCl	726 ± 15			
GTP - NaCl	109 ± 3	50	107	
GTP + 100 mM NaCl	575 ± 13			2000
GTP + 100 mM KCl	732 ± 33			
UK 14304, steady state	74 ± 1[b]	65	52	
UK 14304, pre steady state	6 ± 1[b]	64	4	

[a] Experimental EC_{50} values for epinephrine and GTP are from dose–response curves in the absence and presence of 100 mM NaCl. EC_{50} values for UK 14304 in steady-state and pre-steady-state inhibition of adenylate cyclase are from Thomsen et al. (1988). Experimental data are expressed as mean ± SEM. Theoretical EC_{50} values are from simulations of dose–response curves according to our model using parameter sets B, C, and D (see Table II). [b] From Thomsen et al. (1988).

Influence of Monovalent Ions on Steady-State Inhibition of Adenylate Cyclase by Epinephrine. The effect of NaCl and KCl on the epinephrine concentration dependence of steady-state inhibition was determined (Table I). In the absence of ion, an EC_{50} of 55 ± 2 nM and a maximal inhibition of 30% were obtained. One hundred millimolar NaCl resulted in a 29-fold increase of the EC_{50} to 1.6 ± 0.03 μM, and maximal inhibition was 36%. One hundred millimolar KCl increased the EC_{50} of epinephrine by 13-fold to 726 ± 15 nM with a maximal inhibition of 33%. These results suggest that monovalent ions only weakly increase the fractional inhibition of adenylate cyclase but greatly alter agonist potency. Forty millimolar NaCl produces a half-maximal increase in the EC_{50} for epinephrine (Thomsen 1989).

Influence of Monovalent Ions on GTP Support of Epinephrine-Mediated Inhibition of Adenylate Cyclase. In the absence of epinephrine and monovalent ions, high concentrations of GTP alone inhibit adenylate cyclase by 32% (Figure 6A). One hundred micromolar GTP produces 28% inhibition in the presence of 100 mM KCl but only 5% inhibition in the

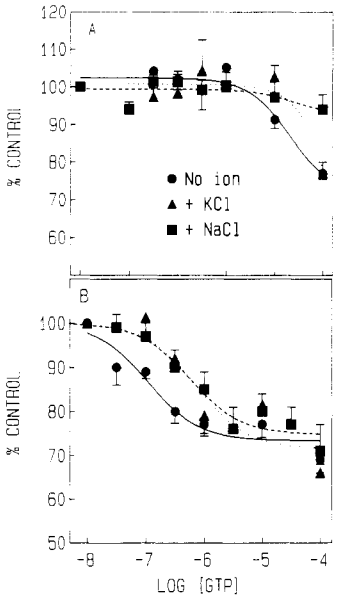

FIGURE 6: Influence of NaCl and KCl on GTP support of epinephrine-mediated inhibition of adenylate cyclase. Steady-state inhibition of forskolin-stimulated adenylate cyclase (A) without and (B) with 10 μM epinephrine in the absence of ion (●) and in the presence of 100 mM NaCl (■) or KCl (▲) is shown. All reactions were in 100 μL and contained 0.05–0.1 mg of protein/tube and other reagents described under Materials and Methods. Data are expressed as percent control which is based on the adenylate cyclase activity observed in the absence of added GTP. Each data point represents the mean ± SEM of five (no ion) and three (+NaCl or KCl) separate experiments in which triplicate determinations were made at each GTP concentration. Curves represent a nonlinear least-squares fit of the data using the computer curve-fitting program described under Materials and Methods.

presence of 100 mM NaCl. Thus, NaCl but not KCl reduces inhibition by GTP alone.

Without exogenous GTP, epinephrine-mediated inhibition is minimal (Figure 6B), indicating that our platelet plasma membrane preparations contain low levels of endogenous guanine nucleotides. Addition of 100 mM NaCl increased the EC_{50} for GTP from 109 ± 3 to 575 ± 13 nM whereas 100 mM KCl increased the EC_{50} to 732 ± 33 nM. The maximal levels of inhibition with no addition, 100 mM NaCl, and 100 mM KCl were 27, 26, and 29%, respectively. These results indicate that sodium chloride and potassium chloride also decrease the potency of GTP to support epinephrine-mediated inhibition without altering the maximal response.

Simulations of Agonist-Mediated Inhibition of Adenylate Cyclase. We used our recently described kinetic model of α_2-agonist-mediated inhibition of adenylate cyclase (Thomsen et al., 1988; Figure 1) to fit both the kinetic and steady-state data. It is based on the ternary complex model described for stimulation of adenylate cyclase by β-agonists (DeLean et al., 1980; Stadel et al., 1981). Explicit rate constants are included for each step in the pathway to allow theoretical simulations of the time course of α_2-agonist-mediated G protein activation.

The parameters used for initial simulations were the same as in our previous report on steady-state and pre-steady-state agonist dose–reponse functions (Thomsen et al., 1988; set A, Table II). These parameters were based on kinetic studies of the binding of the selective full agonist [^{3}H]UK 14 304 (Neubig & Thomsen, 1987; Neubig et al., 1988) and parameters for G protein activation and deactivation taken from the literature (Higashijima et al., 1987b; Brandt & Ross, 1986). The rate parameters for [^{3}H]UK 14 304 were used because the kinetics of epinephrine binding have not been measured in detail. However, the equilibrium binding properties and

Table II: Theoretical Rate Parameter Sets[a]

parameter	set A	set B	set C	set D
k_1 (M^{-1} s^{-1})	5.0×10^6	5.0×10^6	5.0×10^6	5.0×10^6
k_{-1} (s^{-1})	0.5	0.5	0.5	10.0
k_2[G] (s^{-1})	0.1	0.1	0.1	0.1
k_{-2} (s^{-1})	0.1	0.1	0.1	0.1
k_3 (s^{-1})	0.1	0.1	5.0	5.0
k_{-3} (s^{-1})	1.0×10^{-4}	1.0×10^{-4}	1.0×10^{-4}	1.0×10^{-4}
k_4 (M^{-1} s^{-1})	1.0×10^7	5.0×10^6	5.0×10^6	5.0×10^6
k_{-4} (s^{-1})	0.1	1.0	1.0	55.0
k_5 (s^{-1})	0.05	1.0	0.1	1.0
k_6 (s^{-1})	0.1	2.0	2.0	2.0

[a] The values of rate parameters for fitting the model in Figure 1 are compared. Set A from Thomsen et al. (1988) was used as the starting parameter set from which the best-fitting values in sets B and C were determined. Sets B and C have k_3 (GDP release) and k_5 (G protein activation), respectively, as their rate-limiting steps. Data obtained in the presence of 100 mM NaCl were best fit by parameter set D.

dissociation kinetics of epinephrine and [^{3}H]UK 14 304 are very similar (U'Prichard et al., 1983; Neubig et al., 1985; Kim & Neubig, 1987). Simulations for 10 μM epinephrine and 100 μM GTP with parameter set A gave a maximal rate constant for G*–GTP formation of 0.05 s^{-1}. This is significantly lower than the value of 0.12–0.16 s^{-1} observed experimentally in the absence of NaCl. Therefore, the rate parameters for steps in the model were varied to determine if a better agreement between experimental and theoretical data could be achieved. The optimal fit was determined by comparing the sum of the squared residuals (SSR) for the different models provided by the SAAM 29 kinetic modeling program. To obtain maximal constraints on the many parameters of the model, all data were fit simultaneously. This includes the kinetics of inhibition with four to six different GTP concentrations as well as steady-state epinephrine and GTP dose–response data (see Table I and Figure 6). The values of k_1, k_{-1}, k_2[G], and k_{-2} were obtained from our previous study (Thomsen et al., 1988), and these values were kept constant in our simulations.

Two different parameter sets (B and C in Table II) gave theoretical predictions that were in reasonable agreement with experimental data (Figure 5, solid curve). For both models, the rate constants for GTP binding (k_4) and dissociation (k_{-4}) were 5×10^6 M^{-1} s^{-1} and 1.0 s^{-1}, respectively. These values give a calculated K_d for this step of 200 nM, which is similar to the experimental EC_{50} value for GTP support of α_2-agonist-mediated inhibition. Since the maximal k_{inh} in the absence of NaCl is between 0.12 and 0.16 s^{-1}, one of the rate constants in the model would be expected to have a similar rate. In the first parameter set (B, Table I), the release of GDP from G protein (k_3, 0.1 s^{-1}) is the slowest forward step. With this low value of k_3, the rates of G protein activation (k_5) and GTP hydrolysis (k_6) had to be increased to 1.0 and 2.0 s^{-1}, respectively, to obtain a rate of inhibition near that observed experimentally (0.12–0.16 s^{-1}). In the second set of rate parameters (C, Table II), dissociation of the DRG–GTP complex and the associated activation of G protein is the slowest forward step rather than GDP release. Thus, the only difference between the two models is that the slow step in B is GDP release (k_3) while in model C it is G protein activation (k_5). Parameter sets B and C gave virtually the same minimum sum of the squared residuals (1.46×10^3 vs 1.38×10^3). This is much less than that for our initial parameter set A (8.72×10^3). In addition to fitting the transient kinetic data, both models B and C account well for the steady-state EC_{50}'s for epinephrine and GTP (Table I).

Since models B and C fit the steady-state and transient kinetics data identically, we looked for ways to distinguish

between the two models. We recently showed that preincubation of platelet membranes with the α_2-agonist UK 14 304 in the absence of GTP greatly increased agonist potency in a 15-s pre-steady-state assay of adenylate cyclase inhibition (Thomsen et al., 1988). In the preincubation protocol, the GDP should dissociate, leaving behind nucleotide-free DRG. Thus, this protocol gives us information about k_4 and k_5 without the confounding influence of k_3. In contrast, the rapid kinetic results are dependent on k_3, k_4, and k_5, so the parameters cannot be examined separately. Consequently, we simulated steady-state and pre-steady-state experiments using the two parameter sets B and C. Only set C correctly predicted the enhanced potency with agonist preincubation, while set B gave similar EC_{50} values for the simulations with and without preincubation (Table I). Thus model C, in which G protein activation is rate limiting, accounts best for all of the data.

The effects of NaCl both on steady-state inhibition and on the kinetics of inhibition can be easily accommodated by our model. A minimum of three parameters must be changed from either set B or set C to fit the experimental data. First, an increase in the rate of dissociation of agonist from receptor (k_{-1}) was required to account for the reduction in steady-state potency of epinephrine to mediate inhibition.[2] An increase in k_{-1} from 0.5 to 10.0 s^{-1} resulted in a 20–30-fold reduction in potency of epinephrine in the simulations (Table I). Second, an increase in the rate of dissociation of GTP from G protein (k_{-4}) from 2.0 to 55.0 s^{-1} accounted for the reduction in the potency of GTP to suport epinehrine-mediated inhibition (Figure 6) and the shift in the relation of k_{inh} and GTP in the presence of NaCl (Figure 5).[2] Third, an increase in the rate constant for the rate-limiting step (k_3 for model B or k_5 for model C) increased the theoretical k_{inh} at higher GTP concentrations to values similar to those observed experimentally in the presence of NaCl (Figure 5). These changes to parameter sets B and C resulted in a single model for the sodium chloride results (set D, Table II). Additional variations in the values of k_{-1}, k_3, k_4, k_{-4}, k_5, and k_6 from those listed did not reduce the sum of the squared residuals (data not shown). The dashed curve in Figure 5 shows theoretical k_{inh} values obtained from simulations using set D. The strong dependence of k_{inh} on GTP concentration and the marked increase in the maximal rate of inhibition with NaCl are predicted from the changes in the rate parameters. Thus, sodium chloride markedly increases the rate-limiting step in adenylate cyclase inhibition, which for model C is the conformational change accompanying activation of the DRG–GTP complex to G*–GTP.

Discussion

A novel rapid-mix quench method has been used to measure the kinetics of adenylate cyclase stimulation and inhibition on the subsecond to second time scale. Our results indicate that activation of G_s and G_i in platelet plasma membranes is much faster than previously reported for reconstituted systems (Brandt & Ross, 1986; Tota et al., 1987). Also, the rate-limiting step in this model of receptor-mediated G protein activation is the G protein conformational change not GDP release.

Our measurements of the rapid kinetics of α_2-agonist-mediated inhibition of adenylate cyclase represent the first kinetic analysis of the regulation of adenylate cyclase by the natural nucleotide regulator GTP on a subsecond to second time scale. The virtually instantaneous stimulation of adenylate cyclase by PGE_1 and forskolin shows that the lag in α_2-agonist-mediated inhibition is not due to limited accessibility of GTP or the [^{32}P]ATP substrate. The lag in inhibition thus provides a kinetic handle on the rate-limiting step in the agonist-mediated inhibitory pathway. The hyperbolic relation between the rate of onset of inhibition, k_{inh}, and GTP concentration provides strong kinetic evidence that a step distal to GTP binding is rate limiting. This dependence of k_{inh} on GTP concentration is especially evident in the presence of NaCl.

We have used our kinetic model of α_2-receptor-mediated inhibition of adenylate cyclase (Thomsen et al., 1988) to analyze the mechanism of GTP and NaCl effects on epinephrine-mediated inhibition. Only model C, in which the conformational change of DRG–GTP to active G*-GTP is rate limiting, accounted for all of our data including our previous agonist preincubation results (Thomsen et al., 1988). To obtain the greater agonist potency observed with agonist preincubation, k_5 or k_6 must be slow to allow accumulation of activated G protein. If k_5 and k_6 were fast, the DRG which accumulated during preincubation would rapidly dissipate, and preincubation would make no difference. For this reason (and see discussion of NaCl data below), we conclude that the G protein activation step, rather than GDP release is rate limiting. Although it has been suggested that release of GDP is the rate-limiting step in regulation of adenylate cyclase (Cassel & Selinger, 1977a–c, 1978; Brandt & Ross, 1985, 1986; Higashijima et al., 1987a,b) our conclusion is in agreement with that of Birnbaumer et al. (1980) which was based on the observation that different guanine nucleotide analogues have different lag periods for stimulation of adenylate cyclase. Some of the disagreement in the literature may arise from the fact that there are different mechanisms for G protein activation by nucleotide alone and for receptor-catalyzed G protein activation. Our data all relate to receptor-catalyzed G protein activation.

The quantitative determination of rate parameters in such a complex model is difficult. Several steps were taken here to reduce uncertainty in the analysis. First, the agonist binding parameters (k_1, k_{-1}, k_2[G], and k_{-2}) were determined from our own studies of the kinetics of binding of [^{3}H]UK 14 304 (Thomsen et al., 1988). Second, both transient kinetics and steady-state responses were measured over a wide range of GTP concentrations, and the steady-state responses at different agonist concentrations. Finally, all of these data were fit simultaneously in order to maximally constrain the parameters.

The rates of G protein activation (1 s^{-1}) and GTP hydrolysis (2 s^{-1}) in our model are much faster than those measured by Brandt and Ross (1986) for G_s reconstituted with β-adrenergic receptors and by Tota et al. (1987) for muscarinic receptor activation of G_i (approximately 1–4 min^{-1} or 0.016–0.06 s^{-1}). These lower values from reconstituted systems would predict lags in agonist responses with half-times of 10–40 s. The faster rate of onset of inhibition seen here requires that G protein *deactivation* be at least as fast as the maximal k_{inh} (0.57 s^{-1}). This is true because *the rate at which a particular chemical species approaches steady state cannot exceed its rate of breakdown* (Neubig, 1990). Thus, the GTPase step (k_6) must be at least as fast as k_{inh} ($\approx$1 s^{-1}), or there must be other mechanisms for deactivation of G*–GTP. Rates of receptor-mediated G protein activation in the range of 1 s^{-1} have also been reported for the rhodopsin–transducin system (Sitaramayya et al., 1988; Wagner et al., 1988) and for muscarinic receptor activation of K^+ channels from bullfrog (Bre-

[2] The effect of 100 mM NaCl to decrease the potency of both epinephrine and GTP could also be accounted for by *decreases* in the association rate constants k_1 and k_4, respectively.

itwiser & Szabo, 1988) and guinea pig (Okabe et al., 1989) heart.

Sodium chloride has three effects on α_2-receptor-mediated inhibition of platelet membrane adenylate cyclase. Gierschik et al. (1988) have discussed two of these: the reduction of agonist potency and the increased concentrations of guanine nucleotide required for inhibition. The effect of sodium chloride on the maximal rate of adenylate cyclase inhibition is novel and could only be studied by the rapid kinetic method. The maximal rate of epinephrine-mediated inhibition of adenylate cyclase is 3-fold higher in the presence of 100 mM NaCl. Also, k_{inh} becomes strongly dependent on GTP concentration. This is not compatible with a kinetic model in which GDP release is rate limiting. Jakobs et al. (1984a,b) have showed that NaCl slowed inhibition of adenylate cyclase by fixed concentrations of *nonhydrolyzable* guanine nucleotide analogues. This apparent discrepancy may be due to (1) the use of fixed analogue concentrations coupled with a reduction in nucleotide potency by NaCl, (2) differences between GTP and the nonhydrolyzable analogues, or (3) differences in the mechanisms of receptor- versus non-receptor-mediated inhibition. Higashijima et al. (1987b) found that sodium chloride *reduced* the rate of dissociation of GTP from detergent extracts of G_o and reduced the rate of hydrolysis of GTP by G_o. Those effects of NaCl were specific for Cl^- ion rather than Na^+ ion. In our model, NaCl *increases* the rate of GTP dissociation from receptor-stimulated G_i. Thus, the effects of an agent on an isolated detergent-solubilized G protein can be very different from those on a membrane-bound receptor-coupled G protein.

Within the context of the kinetic model, the three effects of sodium chloride on kinetic and steady-state data can be accounted for by changing three rate parameters. The effects on ligand potency are easily explained by an increase in the rate of agonist dissociation from receptor (k_{-1}) and GTP dissociation from G protein (k_{-4}). Indeed, NaCl increases the rate of [^{3}H]epinephrine (Limbird et al., 1982) and [^{3}H]UK 14 304 (Thomsen, 1989) dissociation from the α_2-adrenergic receptor. The locus of sodium's effect on α_2-agonist binding appears to reside on the receptor itself (Nunnari et al., 1987). An increase in the rate of G protein activation (i.e., k_5) accounts for the increase in the maximal rate of agonist-mediated inhibition in the presence of NaCl. The ionic specificity of the different effects of sodium chloride suggest at least two distinct sites of action. The site(s) responsible for the effect on agonist and GTP affinity recognize(s) both NaCl and KCl while the site regulating the rate of G protein activation is highly specific for Na^+. Thus, changes in intracellular sodium concentration may alter the efficiency of G_i-coupled processes by speeding the rate-limiting step.

Certain aspects of our approach to identifying the kinetic parameters of G protein activation must be considered. One is the indirect nature of the measurement of G protein activation. If the rate-limiting step in adenylate cyclase activation or inhibition were the interaction of the activated G protein with the catalyst, our estimates of the rate of G protein activation would be incorrect. In that case, however, the G protein activation would actually be faster than the observed adenylate cyclase response. Thus, our estimates of the rates of G_s and G_i activation may be underestimates of the true values. In contrast, a highly efficient coupling of the G protein (e.g., G_s) to the catalyst could result in the rate of activation of adenylate cyclase activity being faster than that of the G protein. This may be considered to be a kinetic analogue of receptor reserve in steady-state dose–response measurements. For the β-adrenergic receptor and G_s-mediated activation of adenylate cyclase, a substantial receptor reserve often exists (Terasaki & Brooker, 1978) and may result in an overestimate of the rate of activation of G_s. This alone, however, seems insufficient to account for the discrepancy between the time constant of greater than 1 s^{-1} observed here and that of 1 min^{-1} observed for the reconstituted system (Brandt & Ross, 1986). In the case of α_2-adrenergic receptors and G_i, the amount of receptor reserve identified is small and would change our estimates of rates by only a factor of 2 or less [Lenox et al., 1985; see footnote 3 in Thomsen et al. (1988)].

In our previous work on the kinetics of α_2-agonist binding to platelet membranes (Neubig et al., 1988), we concluded that approximately one-third of the α_2 receptors cannot couple to G protein, one-third are precoupled to G protein prior to agonist binding, and the other third couple slowly after agonist binding. The uncoupled receptors would not be expected to play any role in the adenylate cyclase responses since they do not interact with the G_i transducer. We might have expected to see evidence of the precoupled receptors as an initial burst of inhibition, but there was no evidence for such a burst. This could be due to the limited precision of the data at the earliest time points. Also, the amount of G_i that could be rapidly activated by precoupled receptors would be one-third the number of receptors present. We have shown that there is a 20–50-fold excess of G_i over α_2 receptor in platelet membranes (Neubig et al., 1985). Since a single receptor can activate at least 4–10 G protein molecules (Brandt & Ross, 1986; Tota et al., 1988), the burst of inhibition might be small compared to the steady-state level of active G_i reached.

Stimulation of platelet adenylate cyclase by PGE_1 in the presence of GTP is instantaneous ($t_{1/2}$ <1 s) even when the rapid-mix quench method is used. This confirms and extends previous manual time course studies of adenylate cyclase stimulation (Birbaumer & Pohl, 1973; Rodbell et al., 1974; Sonne et al., 1978). We have only measured the time course of stimulation in the presence of saturating concentrations of PGE_1 and GTP; thus, it is possible that transient kinetics may be detectable at lower agonist or GTP concentrations. In fact, stimulation of hepatic membrane adenylate cyclase does exhibit transient kinetics in the presence of subsaturating concentrations of glucagon and GTP (Rodbell et al., 1974).

Forskolin-mediated stimulation of platelet membrane adenylate cyclase occurs immediately when studied by the rapid-mix quench method on the 0.5–30-s time scale. Manual time course measurements (Green & Clark, 1982; Thomsen, 1989) show that forskolin stimulation is biphasic with an inflection point at 1–2 min of incubation. The biphasic time course of forskolin stimulation of platelet membrane adenylate cyclase was not influenced by NaCl, KCl, or the concentration of GTP (100 nM–100 μM) included in the adenylate cyclase assay (Thomsen, 1989). Jakobs et al. (1984a) also reported that NaCl had no effect on forskolin-stimulated platelet adenylate cyclase. Adenylate cyclase stimulation by forskolin appears to involve two mechanisms. One is the direct activation of the catalytic subunit of adenylate cyclase (Seamon & Daly, 1981), and the other involves an interaction of G_s and catalytic subunit (Darfler et al., 1982; Green & Clark, 1982; Bouhelal et al., 1985). It is somewhat surprising that there is no effect of GTP concentration on the time course of forskolin-mediated stimulation since G_s appears to be involved. However, it is possible that lowering GTP concentrations below 100 nM may influence the slow phase of stimulation.

A recent report described the time course of isoproterenol- and forskolin-mediated stimulation of C6 glioma cell mem-

brane adenylate cyclase on the subsecond to second time scale using a rapid-mix quench method similar to the one used in this study (Valeins et al., 1988). A transient 1–2-s burst in stimulation was reported for both isoproterenol and forskolin. Those authors proposed that this burst was either due to an endogenous pool of ATP with rapid access to enzyme or due to a preexisting intermediate of the cyclization reaction. It contrast, we did not observe a burst in stimulation by either PGE_1 or forskolin. Valeins et al. (1988) did not mention the GTP concentration in their adenylate cyclase assay which makes it difficult to compare the results from their study and ours. If no exogenous GTP was included, the transient response might be due to depletion of GTP. Two other differences between the studies are that we used purified platelet membranes with [α-^{32}P]ATP as substrate while they used a crude C6 glioma cell membrane preparation and a cAMP radiuoimmunoassay method. Both studies do show that adenylate cyclase stimulation can be quantitated on a subsecond to second time scale.

In summary, rapid kinetic studies of α_2-agonist-mediated inhibition of adenylate cyclase have provided information not accessible by manual time course studies. The rate-limiting step in this process appears to be distal to GDP release and occurs on the second time scale. The combination of rapid kinetic measurements with specific kinetic models can help elucidate the mechanism of receptor-mediated G protein activation.

Acknowledgments

We thank Tom Larmee and Bob Austin for assistance in the design and construction of the rapid-mix quench apparatus, Ki-Hong Noh for the design and programming of the computer interface, and Dave Ballou for advice. John Jacquez and David Foster provided valuable assistance in the use of SAAM 29, Harvey Motulsky made many helpful suggestions regarding presentation, and Denise Watkins helped prepare the manuscript.

References

Birnbaumer, L., & Pohl, S. L. (1973) *J. Biol. Chem. 248*, 2056–2061.

Birnbaumer, L., Swartz, T. L., Abramowitz, J., Mintz, P. W., & Iyengar, R. (1980) *J. Biol. Chem. 255*, 3542–3551.

Bouhelal, R., Guillon, G., Homburger, V., & Bockaert, J. (1985) *J. Biol. Chem. 260*, 10901–10904.

Brandt, D. R., & Ross, E. M. (1985) *J. Biol. Chem. 260*, 266–272.

Brandt, D. R., & Ross, E. M. (1986) *J. Biol. Chem. 261*, 1656–1664.

Breitwieser, G. E., & Szabo, G. (1988) *J. Gen. Physiol. 91*, 469–493.

Casey, P. J., & Gilman, A. J. (1988) *J. Biol. Chem. 263*, 2577–2580.

Cassel, D., & Selinger, Z. (1977a) *Biochim. Biophys. Acta 452*, 538–551.

Cassel, D., & Selinger, Z. (1977b) *Proc. Natl. Acad. Sci. U.S.A. 74*, 3307–3311.

Cassel, D., & Selinger, Z. (1977c) *J. Cyclic Nucleotide Res. 3*, 11–22.

Cassel, D., & Selinger, Z. (1978) *Proc. Natl. Acad. Sci. U.S.A. 75*, 4155–4159.

Cerione, R. A., Regan, J. W., Nakata, H., Codina, J., Benovic, J. L., Gierschik, P., Spiegel, A. M., Birnbaumer, L., Lefkowitz, R. J., & Caron, M. G. (1986) *J. Biol. Chem. 261*, 3901–3909.

Chance, B. (1974) *Tech. Chem. 6*, 5–62.

Darfler, F. J., Mahan, L. C., Koachman, A. M., & Insel, P. A. (1982) *J. Biol. Chem. 257*, 11901–11907.

DeLean, A., Stadel, J. M., & Lefkowitz, R. J. (1980) *J. Biol. Chem. 255*, 7108–7117.

Fersht, A. R., & Jakes, R. (1975) *Biochemistry 14*, 3350–3356.

Florio, V. A., & Sternweis, P. C. (1985) *J. Biol. Chem. 260*, 3477–3483.

Foster, D. M., & Boston, R. C. (1979) in *Compartmental Distribution of Radiotracers* (Robertson, J. R., Ed.) CRC Press, Boca Raton, FL.

Gierschik, P., McLeish, K., & Jakobs, K. H. (1988) *J. Cardiovasc. Pharmacol. 12* (*Suppl. 5*), S20–S24.

Gilman, A. G. (1987) *Annu. Rev. Biochem. 56*, 615–649.

Green, D. A., & Clark, R. B. (1982) *J. Cyclic Nucleotide Res. 8*, 337–346.

Higashijima, T., Ferguson, K. M., Smigel, M. D., & Gilman, A. G. (1987a) *J. Biol. Chem. 262*, 757–761.

Higashijima, T., Ferguson, K. M., & Sternweis, P. C. (1987b) *J. Biol. Chem. 262*, 3597–3602.

Jakobs, K. H. (1979) *Mol. Cell. Endocrinol. 16*, 147–156.

Jakobs, K. H., & Aktories, K. (1983) *Biochim. Biophys. Acta 732*, 352–358.

Jakobs, K. H., Minuth, M., & Aktories, K. (1984a) *J. Receptor Res. 4*, 443–458.

Jakobs, K. H., Aktories, K., & Schultz, G. (1984b) *Adv. Cyclic Nucleotide Res. 17*, 135–143.

Kim, M. H., & Neubig, R. R. (1987) *Biochemistry 26*, 3664–3672.

Lenox, R. H., Ellis, H., Van Riper, D., & Ehrlich, Y. H. (1985) *Mol. Pharmacol. 27*, 1–9.

Limbird, L. E. (1981) *Biochem. J. 195*, 1–13.

Limbird, L. E., Speck, J. L., & Smith, S. K. (1982) *Mol. Pharmacol. 21*, 609–617.

Lowry, O. H., Rosebrough, N. J., Farr, A. L., & Randall, R. J. (1951) *J. Biol. Chem. 193*, 265–275.

May, D. C., & Ross, E. M. (1988) *Biochemistry 27*, 4888–4893.

Neubig, R. R. (1980) Ph.D. Thesis, Harvard University, Cambridge, MA.

Neubig, R. R. (1990) in *Principles of Drug Action* (Pratt, W. B., & Taylor, P., Eds.) Chapter 4, Churchill Livingstone, New York (in press).

Neubig, R. R., & Szamraj, O. (1986) *Biochim. Biophys. Acta 854*, 67–76.

Neubig, R. R., & Thomsen, W. J. (1987) in Membrane Proteins: Proceedings of the Membrane Symposium, pp 619–632, August 3–6, 1986, San Diego, CA.

Neubig, R. R., Boyd, N. D., & Cohen, J. B. (1982) *Biochemistry 21*, 3460–3467.

Neubig, R. R., Gantzos, R. D., & Brasier, R. S. (1985) *Mol. Pharmacol. 28*, 475–486.

Neubig, R. R., Gantzos, R. D., & Thomsen, W. J. (1988) *Biochemistry 27*, 2374–2384.

Nunnari, J. M., Repaske, M. G., Brandon, S., Cragoe, E. J., & Limbird, L. E. (1987) *J. Biol. Chem. 262*, 12387–12392.

Okabe, K., Yatani, A., & Brown, A. M. (1989) *Biophys. J. 55*, 586a.

Rodbell, M., Lin, M. C., & Salomon, Y. (1974) *J. Biol. Chem. 249*, 59–65.

Salomon, Y., Londos, C., & Rodbell, M. (1974) *Anal. Biochem. 58*, 541–548.

Seamon, K., & Daly, J. W. (1981) *J. Biol. Chem. 256*, 9799–9801.

Sitaramayya, A., Casadevall, C., Bennett, N., & Hakki, S. I. (1988) *Biochemistry 27*, 4880-4887.
Sonne, O., Berg, T., & Christoffersen, T. (1978) *J. Biol. Chem. 253*, 3203-3210.
Stadel, J. M., DeLean, A., & Lefkowitz, R. J. (1982) *Adv. Enzymol. Relat. Areas Mol. Biol. 53*, 1-43.
Steer, M. L., & Wood, A. (1979) *J. Biol. Chem. 254*, 10791-10797.
Terasaki, W. L., & Brooker, G. (1978) *J. Biol. Chem. 253*, 5418-5425.
Thomsen, W. J. (1989) Ph.D. Thesis, University of Michigan, Ann Arbor, MI.
Thomsen, W. J., Jacquez, J. A., & Neubig, R. R. (1988) *Mol. Pharmacol. 34*, 814-822.
Tolkovsky, A. M., & Levitzki, A. (1978) *Biochemistry 17*, 3795-3810.
Tolkovsky, A. M., Braun, S., & Levitzki, A. (1982) *Proc. Natl. Acad. Sci. U.S.A. 79*, 213-217.
Tota, M. R., Kahler, K. R., & Schimerlik, M. I. (1987) *Biochemistry 26*, 8175-8182.
U'Prichard, D. C., Mitrius, J. C., Kahn, D. J., & Perry, B. D. (1983) in *Molecular Pharmacology of Neurotransmitters* (Segawa, T., Yamamura, H. I., & Kuriyama, K., Eds.) pp 53-72, Raven Press, New York.
Valeins, H., Volker, T., Viratelle, O., & Labouesse, J. (1988) *FEBS Lett. 226*, 331-336.
Wagner, R., Ryba, N., & Uhl, R. (1988) *FEBS Lett. 234*, 44-48.

Construction of an Artificial Bifunctional Enzyme, β-Galactosidase/Galactose Dehydrogenase, Exhibiting Efficient Galactose Channeling†

Peter Ljungcrantz,§ Helén Carlsson,§ Mats-Olle Månsson,§ Peter Buckel,‡ Klaus Mosbach,§ and Leif Bülow*,§

Pure and Applied Biochemistry, Chemical Center, POB 124, S-221 00 Lund, Sweden, and Boehringer Mannheim GmbH, Nonnenwald 2, D-8122 Penzberg, FRG

Received May 1, 1989; Revised Manuscript Received July 10, 1989

ABSTRACT: The in-frame fusion between two oligomeric enzymes, β-galactosidase and galactose dehydrogenase, is described. The *lacZ* gene was fused to the 3′ end of the *galdh* gene with a linker encoding only three amino acids. The purified artificial bifunctional enzyme displayed the enzymic activity of both gene products. The hybrid protein was found in two major forms, consisting of four and six subunits, but other forms could also be identified. The molecular weight of each subunit was determined to be 145 000 by sodium dodecyl sulfate–polyacrylamide gel electrophoresis. The bifunctional enzyme shows kinetic advantages over the identical native system in conversion of lactose to galactonolactone. A higher steady-state rate and a reduction of the transient time are observed. This phenomenon is especially pronounced at low initial substrate concentrations and when the pH is adjusted to a level at which the galactose dehydrogenase activity is much higher than that of the β-galactosidase.

Over the years, we have devoted much attention to the study of the proximity effects of sequentially operating enzymes. Much of this work has been focused on the use of immobilization and cross-linking technologies (Mosbach & Mattiasson, 1970; Srere et al., 1973; Srere & Mosbach, 1974; Månsson et al., 1983). Another approach to the investigation of these effects has been our attempts to prepare artificial bifunctional enzymes by gene fusion. We have previously fused β-galactosidase and galactokinase to form a hybrid protein carrying both activities in order to obtain a better understanding of the microenvironmental effects caused by the proximity of the two catalytic entities (Bülow et al., 1985). The intermediate product, galactose, was more efficiently transferred to the second enzyme in the reaction sequence in an assay medium with a viscosity similar to that found in vivo (Bülow, 1987). These latter studies in a sense also initiate the investigation of the spatial organization of enzymes in relation to each other that has proved to be essential in many metabolic sequences and cycles. However, enzymes of different biological origin which catalyze the same reaction sequence represent a variety of gene arrangements, as illustrated by the presence of individual enzymes, multienzyme complexes, and multifunctional enzymes (Welch, 1985). Therefore, the hypothesis was put forward early that bi- and multifunctional enzymes have evolved through gene fusion (Mowbray & Moses, 1976), a hypothesis that later has been strengthened experimentally through comparison of DNA sequences (Zalkin et al., 1984).

In the present study, we have extended our investigation of artificial bifunctional enzymes to include the design and preparation of a hybrid protein consisting of two naturally occurring oligomeric enzymes. The structural gene of β-galactosidase (*Escherichia coli*), a tetrameric enzyme, was thus ligated to the 3′ end of the gene of galactose dehydrogenase (*Pseudomonas fluorescens*), a dimeric enzyme (Blachnitzky et al., 1974). These enzymes catalyze the sequential hydrolysis of lactose followed by the oxidation of the galactose formed to the corresponding lactone:

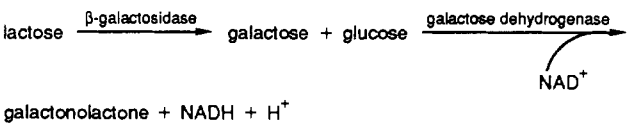

† This project was supported by grants from the Swedish Board for Technical Development to K.M.
§ Chemical Center.
‡ Boehringer Mannheim GmbH.

0006-2960/89/0428-8786$01.50/0